Energy dispersion, superconductivity, and magnetic fluctuations in stacked altermagnetic materials

Jun Chang [1,*] Hantao Lu [2,3,†] Jize Zhao,[3,4] Hong-Gang Luo,[3,4] and Yang Ding[5]

[1]*School of Physics and Information Technology, Shaanxi Normal University, Xi'an 710119, China*

[2]*Key Laboratory of Quantum Theory and Applications of MoE, Lanzhou University, Lanzhou 730000, China*

[3]*Lanzhou Center for Theoretical Physics, Key Laboratory of Theoretical Physics of Gansu Province, Lanzhou University, Lanzhou 730000, China*

[4]*School of Physical Science and Technology & Key Laboratory of Quantum Theory and Applications of MoE, Lanzhou University, Lanzhou 730000, China*

[5]*Center for High-Pressure Science and Technology Advanced Research, Beijing 100094, China*

(Received 28 October 2024; revised 7 March 2025; accepted 11 March 2025; published 26 March 2025)

Recently, altermagnetism (AM) has emerged as a new category of magnetism, alongside conventional antiferromagnetism (AFM) and ferromagnetism. In an AM, superconductivity (SC) is faced with a dilemma that the spin-polarized bands, induced by the broken time reversal ($\mathcal{T}$) symmetry, dominantly support spin-triplet pairing. In contrast, AM spin fluctuations routinely facilitate spin-singlet pairing as in AFM. Consequently, unconventional SC is either absent or weak in AM materials. Here, we propose that stacking two-dimensional (2D) AM materials could resolve this dilemma. Stacked 2D materials have yielded a variety of new electronic properties by altering the symmetries inherent in the monolayer. In a 2D anisotropic Hubbard model, we investigate the general energy dispersions of both single-layer and stacked AM materials. We demonstrate that AM sheet stacking can alter the original symmetries, consequently affecting the energy dispersion. The interlayer magnetic coupling enhances the low $\mathbf{q}$ magnetic fluctuations. $\mathcal{T}$ symmetry is restored in the AA stacking with an antiferromagnetic interlayer coupling and then both the energy dispersion and pairing interaction are in favor of spin-singlet SC. The ferromagnetic interlayer coupling in the AB stacking not only recovers $\mathcal{T}$ symmetry but also supports spin-triplet pairing. It is further anticipated that twisted bilayer AM sheets could exhibit additional novel electronic properties, including topology, flat bands, and collective excitations. Our work illustrates that stacking sheets of AM materials could open up a unique research domain in exploring novel quantum phenomena and offer a fertile ground for potential electronic applications.

DOI: 10.1103/PhysRevB.111.104432

I. INTRODUCTION

A recently identified category of magnetism, referred to as altermagnetism (AM), has been extensively studied due to its distinct properties and potential applications [1–8]. It exhibits a zero net magnetization, akin to conventional antiferromagnetism (AFM), and spin-splitting energy dispersion similar to ferromagnetism (FM) in the reciprocal momentum space. Owing to their significant fundamental and technological significance, extensive theoretical and experimental research has been conducted on these captivating magnets. A variety of unique electromagnetic phenomena have been theoretically predicted, including spin-dependent band splitting and anomalous Hall and Kerr effects [9–13], as well as spin current and torque [14–19], and substantial tunneling magnetoresistance effects [20]. Meanwhile, materials hypothesized to exhibit antiferromagnetic properties have been the subject of experimental inquiries, such as RuO_2 [2,21–24], $FeSb_2$ [25], MnF_2 [6,26,27], MnTe [28–30], Mn_5Si_3 [31], CrSb [32], and La_2CuO_4 [2].

The emergence of superconductivity (SC) in AM has garnered immediate interest [33–42]. A defining characteristic of AM is the broken translation or inversion symmetry between the two magnetic sublattices besides the antiparallel magnetization. Owing to the alternating spin polarization in real space, the superconducting condensate in AM remains nonmagnetic, similar to that in AFM. Unlike AFM, the AM structure, similar to FM, breaks the $\mathcal{T}$ symmetry and eliminates the spin degeneracy of the electronic energy bands, resulting in $\varepsilon(\mathbf{k},\uparrow) \neq \varepsilon(-\mathbf{k},\downarrow)$. On one hand, near the Fermi energy levels, spin-polarized electrons with antiparallel momenta tend to form spin-triplet Cooper pairs, as is typical in FM. On the other hand, the superconducting pairing interaction is frequently ascribed to magnetic fluctuations in both AFM and FM, which support spin-singlet and spin-triplet SC, respectively. Given that the AM order typically deviates only slightly from AFM, the spin fluctuation spectra in AM closely resemble those in AFM [33,43]. Consequently, the SC induced by AM magnetic fluctuations is expected to be predominantly characterized by spin-singlet pairing. This conflict between the pairing interactions and the electronic structure could potentially lead to the absence or weakness of SC in AM. Despite the potential for magnetic fluctuations at low $\mathbf{q}$, arising from scattering between different spin-polarized

*Contact author: junchang@snnu.edu.cn

†Contact author: luht@lzu.edu.cn

bands, to support spin-triplet SC in AM, the typically weak spectral weight of these fluctuations at low **q** results in substantially weaker spin-triplet pairing [43].

In this study, we concentrate on the energy dispersion of 2D AM materials. A general anisotropic Hubbard model, incorporating an on-site Coulomb repulsion denoted by U, is investigated. Utilizing the on-site mean field approximation, we derive the energy dispersion. The unconventional superconducting pairing is ascribed to the short-range magnetic interactions among electrons. In a single layer, the energy band is spin split due to the broken $\mathcal{T}$ symmetry by the AM order; thus spin-singlet Cooper pairs with $\mathcal{T}$ symmetry are not favored. On the other hand, AM spin fluctuations typically resemble those in AFM, favoring spin-singlet pairing. We propose that stacking AM sheets in some patterns can restore the broken $\mathcal{T}$ symmetry in AM materials, thereby supporting the formation of spin-singlet Cooper pairs. The interlayer magnetic coupling strengthens the low **q** magnetic fluctuations. Stacking sheets of 2D materials alters the original symmetries of the individual layers [44–46] and endows them with a variety of new electronic properties [47–52]. Furthermore, when the layers are twisted relative to each other at an angle, the resulting superlattice exhibits a significantly larger periodicity than the individual layer, thereby possessing complex and rich electronic properties, such as superconductivity, correlated insulating states, and flat electronic bands. We anticipate that stacked 2D AM materials will pave new avenues for both fundamental research and potential applications. The capability to modulate electronic properties through twist angle variation and external field application further constitutes a crucial platform for investigating novel quantum phenomena in AM.

II. SINGLE LAYER AM MODEL

Initially, to investigate the properties of a single AM sheet, we construct a 2D Hubbard model with the Hamiltonian

$$H = -\sum_{ij\sigma}(t_{ij} + \mu\delta_{ij})c^{\dagger}_{i\sigma}c_{j\sigma} + U\sum_{i} n_{i\uparrow}n_{i\downarrow}, \tag{1}$$

where $c^{\dagger}_{i\sigma}$ and $c_{i\sigma}$ are the electron creation and annihilation operators with spin σ on site i. $n_{i\sigma} = c^{\dagger}_{i\sigma}c_{i\sigma}$ represents the corresponding particle number operators. Furthermore, t_{ij} denotes the single-particle hopping integral between site i and j. U represents the on-site Coulomb repulsion, while μ is the chemical potential.

For the interaction term of Eq. (1), we initially ignore the fluctuations in particle number and subsequently apply the mean field decoupling [43],

$$U n_{i\uparrow}n_{i\downarrow} \approx U(\langle n_{i\uparrow}\rangle n_{i\downarrow} + n_{i\uparrow}\langle n_{i\downarrow}\rangle - \langle n_{i\uparrow}\rangle\langle n_{i\downarrow}\rangle). \tag{2}$$

Further, the average spin and particle number are defined,

$$S_i \equiv \tfrac{1}{2}\langle n_{i\uparrow} - n_{i\downarrow}\rangle, \quad N_i \equiv \langle n_{i\uparrow} + n_{i\downarrow}\rangle. \tag{3}$$

The mean field Hamiltonian is written as

$$H_{\mathrm{mf}} = -\sum_{ij\sigma}(t_{ij} + \mu\delta_{ij} + \sigma U S_i\delta_{ij})c^{\dagger}_{i\sigma}c_{j\sigma}, \tag{4}$$

where UN_i has been absorbed into the chemical potential and the constant term $U\langle n_{i\uparrow}\rangle\langle n_{i\downarrow}\rangle$ is neglected. To characterize AM, the lattice is partitioned into A and B sublattices, featuring distinct intrasublattice (AA and BB) hopping terms. By setting the chemical potential μ to zero, the Fourier transformation of the mean field Hamiltonian into reciprocal space yields

$$H_{\mathrm{mf}} = -\sum_{aa'\mathbf{k}\sigma}\varepsilon_{aa'}(\mathbf{k},\sigma)c^{\dagger}_{a\mathbf{k}\sigma}c_{a'\mathbf{k}\sigma}, \tag{5}$$

where $\mathbf{k}$ is the crystal momenta of a sublattice, a and a' belong to sublattice A or B, and the matrix elements of the Hamiltonian are given by

$$\varepsilon_{aa'}(\mathbf{k},\sigma) = \epsilon_{aa'}(\mathbf{k}) + \sigma U S_a\delta_{aa'}, \tag{6}$$

where $\sigma = \pm 1$ for spin up and down, respectively, and $\epsilon_{aa'}(\mathbf{k})$ represents the spin independent matrix elements, determined by the lattice structure and the hopping integrals between sublattices a and a'. The nature of Eq. (6) is highly sensitive to the hopping integrals t_{ij}, the mean spin values S_A and S_B on the two sublattices. When there is no net magnetization on either sublattice, or $S_A = S_B = 0$, it is a paramagnetic (PM) state. A ferromagnetic state is realized when both sublattices have the parallel alignment magnetization or $S_A = S_B \neq 0$. The antiferromagnetic state emerges when there is translation or inversion symmetry between the two antiparallel magnetic sublattices with $S_A = -S_B \neq 0$. Lastly, an altermagnetic state requires the breaking of translation and inversion symmetry between the two antiparallel magnetic sublattices. This can be achieved through anisotropic hopping constants or a rotation symmetry between the two sublattices, along with nonzero magnetizations. In AM materials, it is assumed that the electron density is uniform with $N_A = N_B$, whereas the spin polarization alternates between sublattices A and B with $S_A = -S_B$. Then, the system energy dispersion is given by

$$\varepsilon^{\mp}(\mathbf{k},\sigma) = \varepsilon_{A+B}(\mathbf{k},\sigma) \mp \sqrt{\epsilon^2_{AB}(\mathbf{k}) + \varepsilon^2_{A-B}(\mathbf{k},\sigma)}, \tag{7}$$

where

$$\varepsilon_{A\pm B}(\mathbf{k},\sigma) \equiv \tfrac{1}{2}[\varepsilon_{AA}(\mathbf{k},\sigma) \pm \varepsilon_{BB}(\mathbf{k},\sigma)]$$

and

$$\epsilon_{A\pm B}(\mathbf{k}) \equiv \tfrac{1}{2}[\epsilon_{AA}(\mathbf{k}) \pm \epsilon_{BB}(\mathbf{k})].$$

With the aid of Eq. (6), $\varepsilon_{A+B}(\mathbf{k},\sigma) = \epsilon_{A+B}(\mathbf{k})$ is spin independent and $\varepsilon_{A-B}(\mathbf{k},\sigma) = \epsilon_{A-B}(\mathbf{k}) - \sigma h$ is spin dependent, where $h = US_A$. Then the system energy dispersion in Eq. (7) is rewritten as

$$\varepsilon^{\mp}(\mathbf{k},\sigma) = \epsilon_{A+B}(\mathbf{k}) \mp \sqrt{\epsilon^2_{AB}(\mathbf{k}) + [\epsilon_{A-B}(\mathbf{k}) - \sigma h]^2}. \tag{8}$$

Given that $\epsilon_{aa'}(\mathbf{k})$ exhibits inversion symmetry in the momentum space, i.e., $\epsilon_{aa'}(\mathbf{k}) = \epsilon_{aa'}(-\mathbf{k})$, it follows that the spin-splitting bands $\varepsilon^{\mp}(\mathbf{k},\uparrow) \neq \varepsilon^{\mp}(-\mathbf{k},\downarrow)$ provided that the translation or inversion symmetry between the A and B sublattice is broken, i.e., $\epsilon_{A-B}(\mathbf{k}) \neq 0$, while $\epsilon_{A-B}(\mathbf{k}) = 0$ leads to spin degenerated AFM state. In the absence of spin-orbit interaction, such energy dispersion exclusively supports spin-triplet Cooper pairs with parallel spin order parameter $\Delta_{\sigma\sigma}$ and no coupling exists between the two order parameters $\Delta_{\uparrow\uparrow}$ and $\Delta_{\downarrow\downarrow}$. The spin symmetry between up and down in the AM sublattice ensures the average order parameter unitary [33].

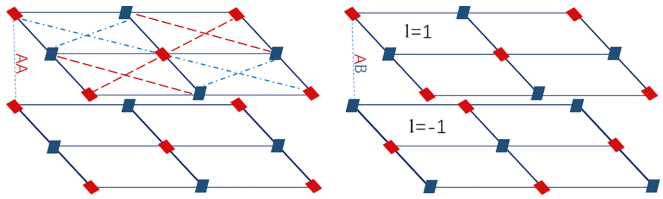

FIG. 1. Schematic of stacking two-dimensional (2D) altermagnetism sheets without a twist angle. The lattice is divided into A (red) and B (blue) sublattices, with distinct hopping integrals between the same-type sublattices. The index $l = 1$ and -1 signify the top and the bottom layers, respectively. Within the same layer, the average spin polarizations on A and B sublattices are antiparallel, with $S_A = -S_B$, whereas across different layers, the spin polarizations may either maintain this antiparallel relationship, $S_A(l = 1) = -S_A(l = -1)$, or align parallel, $S_A(l = 1) = S_A(l = -1)$. The patterns of A-A and B-B stacking are depicted in the left and right panels, respectively.

Equation (8) describes a general energy dispersion relation for anisotropic AFM and AM materials. For AFM materials, there is typically a translation or inversion symmetry between the two sublattices with opposite spins. This symmetry implies that the spin-independent Hamiltonian matrix elements $\epsilon_{aa}(\mathbf{k})$ are identical for both sublattices, i.e., $\epsilon_{AA}(\mathbf{k}) = \epsilon_{BB}(\mathbf{k})$ or $\epsilon_{A-B}(\mathbf{k}) = 0$ for all $\mathbf{k}$. Given this symmetry, the energy dispersions are spin degenerate, $\varepsilon^{\mp}(\mathbf{k}, \sigma) = \epsilon_{A+B}(\mathbf{k}) \mp \sqrt{\epsilon_{AB}^2(\mathbf{k}) + h^2}$. On the other hand, if the translation or inversion symmetry between the A and B sublattices is broken, then there exists $\mathbf{k}$ such that $\epsilon_{A-B}(\mathbf{k}) \neq 0$. In this case, the energy dispersions become spin dependent, which is characteristic of altermagnetism. For example, if the translation or inversion transformation of the A sublattices is followed by a rotation operation and spin reversal operation $\bar{1}$ to reach the B sublattices [53], then the translation or inversion symmetry between the A and B sublattices can be broken. The broken symmetry can lead to differences in the Hamiltonian matrix elements between the two sublattices, specifically, $\epsilon_{A-B}(\mathbf{k}) \neq 0$. This results in spin-dependent energy dispersions. In Fig. 1, the translation transformation of the A sublattices is followed by a $\pi/2$ rotation about the axis perpendicular to the planes and spin reversal $\bar{1}$ to reach the B sublattices. Once the specific geometric structure is defined, the specific type of spin splitting can be determined. Considering the square lattice with two sublattices as an example, the matrix elements of the Hamiltonian are given by [43]

$$\epsilon_{AA}(\mathbf{k}) = -2t_1 \cos 2k_x - 2t_2 \cos 2k_y, \tag{9}$$

$$\epsilon_{BB}(\mathbf{k}) = -2t_2 \cos 2k_x - 2t_1 \cos 2k_y, \tag{10}$$

$$\epsilon_{AB}(\mathbf{k}) = -2t_0(\cos k_x + \cos k_y), \tag{11}$$

where t_0 represents the nearest sublattice A-B hopping amplitude and t_1 and t_2 are the intrasublattice hopping constants that break the sublattice $C4$ symmetry. Adopting the parameters from Ref. [43], with $t_0 = 1$ as the unit of energy, $t_1 = 0.4t_0$, $t_2 = 0.2t_0$, and $U = 3.6t_0$. The corresponding energy band structure, as described in Eq. (8), is depicted in Fig. 2. The four energy bands result from the sublattices and spins. The spin up and down bands are split, depending on the crystal momentum when $t_1 \neq t_2$.

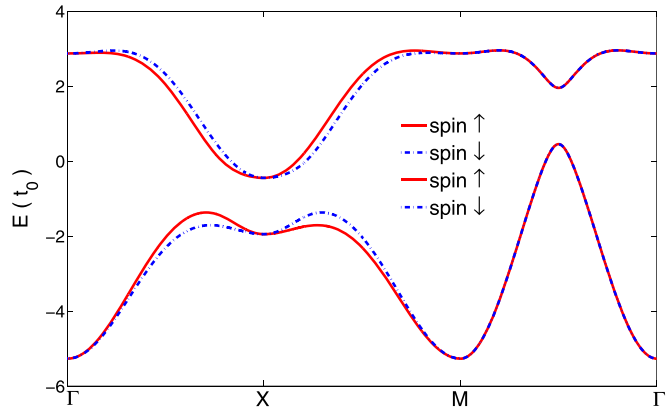

FIG. 2. Metallic AM energy band structure on a square lattice in Eq. (8). Following the parameters in Ref. [43], $t_0 = 1$ as the unit of energy, $t_1 = 0.4t_0, t_2 = 0.2t_0$, and $U = 3.6t_0$. Red and blue bands indicate the spin- ↑ and spin- ↓ components, respectively. The spin splitting is $\mathbf{k}$ dependent. Along $M - \Gamma$, the spin- ↑ and spin- ↓ bands are degenerate. The Fermi surfaces consist of hole pockets at $(\pm\pi/2, \pm\pi/2)$ and electron pockets at $(\pm\pi, 0)$ and $(0, \pm\pi)$ in the reduced Brillouin zone.

In the study of energy dispersion, we focus on the Hubbard model, while, in the study of superconductivity, we turn to the low-energy effective model of the Hubbard model, namely the t-J model. The Heisenberg exchange interaction couples electrons at neighboring sites

$$H_{\text{int}} = \sum_{ij} J_{ij} \mathbf{s}_i \cdot \mathbf{s}_j, \tag{12}$$

where the spin operator $\mathbf{s}_i = c_{i\sigma}^{\dagger}[\boldsymbol{\sigma}]_{\sigma\sigma'} c_{i\sigma'}/2$ with Pauli matrix $\boldsymbol{\sigma} = (\sigma_x, \sigma_y, \sigma_z)$. The pairing order parameters $\Delta_{\sigma\sigma'}$ could stem from the magnetic interaction in Eq. (12) using a mean field method. From the real space point of view, the nearest-neighbor magnetic exchange interaction J_{AB} in the AM state typically favors spin-singlet pairing and the next-nearest-neighbor J_{AA} and J_{BB} support spin-triplet pairing. Nevertheless, the next-nearest-neighbor exchange interactions are typically much weaker than the nearest-neighbor couplings. Therefore, the spin-singlet pairing should be dominant in terms of magnetic interaction. On the other side, the long-range magnetic order and spin fluctuations near $\mathbf{q} \approx 0$ in the AM phase are also possible [33]. Such magnetic fluctuations could support triplet pairing. However, the spectral weight of the spin fluctuations near $\mathbf{q} \approx 0$ in AM is typically quite small, as the AM order often slightly deviates from the AFM order [43]. Consequently, the spin fluctuation dominantly mediates spin-singlet pairing. The contradiction between the electronic structure, favoring spin-triplet pairing, and the pairing interaction, supporting spin-singlet pairing, results in the absence of or weak SC in the AM phase. We tend to alleviate this predicament by stacking AM sheets to alter the electronic structures and spin fluctuation spectra.

III. STACKED LAYER MODEL

Recently, atomically stacking quasi-2D materials results in various superstructures by altering the original geometrical

symmetries inherent in individual layers [47–52]. The artificial superstructure induces a variety of unique electronic properties, including superconductivity, magnetism, topology, correlated insulating states, and flat electronic bands. From a fundamental perspective, the complexity and richness of the electronic properties in stacked 2D materials present significant opportunities to study emergent quantum phenomena. From an application standpoint, stacked 2D materials offer a unique potential for the development of low-power and high-speed electronic devices. Specifically, when two sheets of a 2D material are twisted at the "magic angle," a moire superlattice emerges due to the interference between the two layers. Here, we consider two individual AM layers, designated by $l = \pm 1$. Initially, we disregard the interlayer coupling. When the local magnetic moments on sublattice A are aligned, $S_A(l=1) = S_A(l=-1)$, the energy dispersions mirror those in Eq. (8) for a single layer. Conversely, if the local magnetic moments on sublattice A are in opposition, $S_A(l=1) = -S_A(l=-1)$, then the dispersion is given by

$$\varepsilon^{\mp}(\mathbf{k},\sigma,l) = \epsilon_{A+B}(\mathbf{k}) \mp \sqrt{\epsilon^2_{AB}(\mathbf{k}) + [\epsilon_{A-B}(\mathbf{k}) - l\sigma h]^2}. \tag{13}$$

It is evident that the energy dispersion of the two sheets with opposite spin orientations is identical, i.e., $\varepsilon^{\mp}(\mathbf{k},\uparrow,l=1) = \varepsilon^{\mp}(\mathbf{k},\downarrow,l=-1)$. It is anticipated that the layer coupling could render the system dispersion spin independent.

To unite two layers together, the layer coupling is introduced, such as van der Waals interaction or chemical bonding. It is widely recognized that the energy dispersion of stacked materials is contingent upon the stacking patterns. For simplicity, we restrict our analysis to zero twist angle between sheets and the effective interlayer hopping $t_\perp(il,jl')c^\dagger_{i\sigma l}c_{j\sigma l'}$ is limited to the nearest neighbors, with $t_\perp(il,il') = t_\perp$.

A. AA stacking

The nature of the interlayer magnetic coupling between the stacked sheets, whether ferromagnetic or antiferromagnetic, is dictated by a combination of the magnetic ions and their surrounding ligands, which is encapsulated by the Goodenough-Kanamori-Anderson rule [54–57]. For the AA stacked AM sheets with $S_A(l=1) = -S_A(l=-1)$, the mean field Hamiltonian of this system can be diagonalized exactly and the resulting energy dispersion is characterized by

$$\varepsilon^{\mp}_{\mp}(\mathbf{k},\sigma) = \epsilon_{A+B}(\mathbf{k}) \mp \sqrt{\epsilon^2_{AB}(\mathbf{k}) + \xi^2_{\mp}(\mathbf{k})}, \tag{14}$$

with

$$\xi^2_{\mp}(\mathbf{k}) = \epsilon^2_{A-B}(\mathbf{k}) + t^2_\perp + h^2 \mp 2\sqrt{\epsilon^2_{A-B}(\mathbf{k})(t^2_\perp + h^2) + \epsilon^2_{AB}(\mathbf{k})t^2_\perp}. \tag{15}$$

It is evident that the dispersion is spin independent, with $\varepsilon^{\mp}_{\mp}(\mathbf{k},\uparrow) = \varepsilon^{\mp}_{\mp}(-\mathbf{k},\downarrow)$. The interlayer coupling restores the broken $\mathcal{T}$ symmetry present in the monolayer. This electronic structure, resulting from interlayer coupling, could host spin-singlet Cooper pairs, in contrast to the single AM layer, which only supports spin-triplet SC. Furthermore, the stacking pattern modifies the spin fluctuations. The nearest-neighbor magnetic interaction between two layers is described by

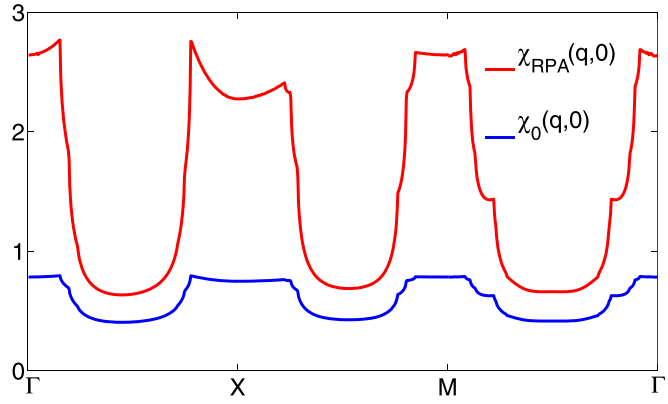

FIG. 3. Bare and RPA magnetic susceptibilities $\chi_0(\mathbf{q},0)$ and $\chi_{\rm RPA}(\mathbf{q},0)$ in the AA stacked AM sheets with $S_A(l=1) = -S_A(l=-1)$. The temperature $T = 0.001t_0$, $t_\perp = 0.2t_0$, and the other parameters are the same as those in Fig. 2. The RPA correction significantly strengthens the spin fluctuations $\chi_{\rm RPA}(\mathbf{q},0)$ around the momenta (0,0), $(\pi,0)$, and (π,π).

$$H_{\rm int} = \sum_{i,l\neq l'} J_{ill'}\mathbf{s}_{il}\cdot\mathbf{s}_{il'}, \tag{16}$$

where the layer index $l, l' = \pm 1$. The interlayer spin coupling within the same unit cell is expected to enhance the low $\mathbf{q}$ spin fluctuations. The susceptibility χ_0 can be expressed by [8,43,58]

$$\chi_{0\sigma\sigma'}(\mathbf{q},\omega) = \sum_{\mathbf{k}} \frac{A_{\mathbf{k},\mathbf{q}}[f(\varepsilon^{\mp}_{\mp}(\mathbf{k},\sigma)) - f(\varepsilon^{\mp}_{\mp}(\mathbf{k}+\mathbf{q},\sigma'))]}{[\omega + i\eta - \varepsilon^{\mp}_{\mp}(\mathbf{k},\sigma) + \varepsilon^{\mp}_{\mp}(\mathbf{k}+\mathbf{q},\sigma')]}, \tag{17}$$

where $A_{\mathbf{k},\mathbf{q}}$ is the coherence factor and f is the Fermi distribution function. Due to the energy band degeneracy $\varepsilon^{\mp}_{\mp}(\mathbf{k},\uparrow) = \varepsilon^{\mp}_{\mp}(\mathbf{k},\downarrow)$, the χ_0 at low $\mathbf{q} \approx \mathbf{0}$ spin fluctuations is dominantly determined by the magnetic scattering processes between the degenerate bands. The magnetic interaction in stacking materials can be decomposed into intralayer and interlayer pairing under the mean field method [59]. The AFM interlayer magnetic fluctuations are capable of mediating s-wave spin-singlet pairing. Thus, in AA stacking with antiferromagnetic coupling between two layers, both electronic structure and spin fluctuations support spin-singlet SC.

Using the same parameters as those for the square lattice with two sublattices in Fig. 2, we investigate the bare and random phase approximation (RPA) magnetic susceptibility of the AA stacked AM sheets with $S_A(l=1) = -S_A(l=-1)$. As depicted in Fig. 3, at the wave vector $\mathbf{Q} = (\pi,\pi)$, the bare susceptibility $\chi_0(\mathbf{Q},\omega=0) = \chi_0(\mathbf{q}=0,\omega=0)$ is proportional to the density of states, which is a consequence of the equality $\varepsilon^{\mp}_{\mp}(\mathbf{k}) = \varepsilon^{\mp}_{\mp}(\mathbf{k}+\mathbf{Q})$. The multiorbital RPA susceptibility matrix can be written as [8]

$$[\chi_{\rm RPA}(\mathbf{q},iq_n)]^{\mu_1,\mu_2}_{\mu_3,\mu_4} = [\chi_0(\mathbf{q},iq_n)[1 - U\chi_0(\mathbf{q},iq_n)]^{-1}]^{\mu_1,\mu_2}_{\mu_3,\mu_4}, \tag{18}$$

where μ_i is the orbital index and iq_n is a bosonic Matsubara frequency, $[U]^{\mu_1,\mu_2}_{\mu_3,\mu_4} = U$ for $\mu_1 = \mu_2 = \mu_3 = \mu_4$. The RPA

correction of the on-site Hubbard interaction primarily amplifies the amplitude of spin fluctuations while subtly modifying the momentum structure. Furthermore, in Fig. 3, the RPA correction significantly boosts the spin fluctuations $\chi_{\rm RPA}(\mathbf{q}, 0)$ around the momenta (0,0), $(\pi, 0)$, and (π, π). The enhancement is expected to favor interlayer SC pairing.

In the AA stacking, if the interlayer coupling is ferromagnetic or $S_A(l = 1) = S_A(l = -1)$, the energy dispersion becomes spin dependent and is given by

$$\varepsilon^{\mp}_{+}(\mathbf{k}, \sigma) = \epsilon_{A+B}(\mathbf{k}) \mp t_\perp \mp \sqrt{\epsilon^2_{AB}(\mathbf{k}) + [\epsilon_{A-B}(\mathbf{k}) - \sigma h]^2}. \tag{19}$$

The interlayer spin coupling significantly enhances the low $\mathbf{q}$ spin fluctuations by interband processes around energy $2t_\perp$ due to $\varepsilon^{-}_{+}(\mathbf{k}, \sigma) = \varepsilon^{+}_{+}(\mathbf{k}, \sigma) + 2t_\perp$. In contrast to the antiferromagnetic interlayer coupling, the ferromagnetic coupling between layers favors s-wave spin-triplet pairing. Consequently, the electronic structure and spin fluctuations both support spin-triplet SC in AA stacking with ferromagnetic interlayer coupling. This distinction underscores the pivotal role of interlayer magnetic coupling in determining the type of superconducting pairing that can emerge in stacked systems.

Applying the decomposition of the Pauli matrix product into spin triplet and singlet configurations,

$$\begin{aligned}\sigma_{\alpha\beta} \cdot \sigma_{\gamma\delta} = &\tfrac{1}{2}(\delta_{\alpha\beta}\delta_{\gamma\delta} + \delta_{\alpha\delta}\delta_{\beta\gamma}) \\ &- \tfrac{3}{2}(\delta_{\alpha\beta}\delta_{\gamma\delta} - \delta_{\alpha\delta}\delta_{\beta\gamma}),\end{aligned} \tag{20}$$

the nearest-neighbor magnetic interaction between two layers in the spin-triplet channel could be written as [60]

$$J_{ll'}\mathbf{s}_l \cdot \mathbf{s}_{l'} \to \frac{J_{ll'}}{4}[n_{l\uparrow}n_{l'\uparrow} + n_{l'\downarrow}n_{l'\downarrow}], \tag{21}$$

where only the same spin interaction terms are kept, as the spin-split bands in AM can only support Cooper pairs with the order parameter $\Delta_{\sigma\sigma}$; see Ref. [33]. The s-wave spin-triplet parameter order in real space is $\Delta_{\sigma\sigma}(i) \sim \langle c_{il\sigma}c_{il'\sigma}\rangle|_{l\neq l'}$ for both sublattices, considering $\mathcal{T}$ symmetry broken by the AM order, and after the Fourier transformation to moment space the pairing amplitudes are given by

$$\Delta^s_{\sigma\sigma} = \frac{J_{ll'}}{4N}\sum_{\mathbf{k}}\langle c_{\mathbf{k}\sigma}c_{-\mathbf{k}\sigma}\rangle(\gamma^{s+is})^*, \tag{22}$$

where the ferromagnetic coupling $J_{ll'} < 0$ and the s-wave gap function factor $\gamma^{s+is} = (1 + i)/\sqrt{2}$, indicating broken $\mathcal{T}$ symmetry. Since SC requires a metallic altermagnetic state, we assume the hole doping away from the Mott insulator is slight and very close to half filling per sublattice. Then in the energy dispersion Eq. (19), only the four lower $\varepsilon^{\mp}_{-}(\mathbf{k}, \sigma)$ bands are occupied. Considering the slight doping, only the top $\varepsilon^{+}_{-}(\mathbf{k}, \sigma)$ bands cross the Fermi energy level and $\epsilon_{AB}(\mathbf{k})$ or the hopping between the A and B sublattice is strongly suppressed by the large Hubbard U. Then

$$\varepsilon^{+}_{-}(\mathbf{k}, \sigma) \approx \epsilon_{A+B}(\mathbf{k}) + \sigma\epsilon_{A-B}(\mathbf{k}) + t_\perp - h.$$

Solving the SC gap Eq. (22) self-consistently, the BCS-like gap equation can be formulated as

$$-\int \frac{d^2k}{4\pi^2}\frac{J_{ll'}}{4E^s(\mathbf{k}, \sigma)}\tanh\frac{\beta E^s(\mathbf{k}, \sigma)}{2} = 1, \tag{23}$$

with the Bogoliubov quasiparticle energy spectra

$$E^s(\mathbf{k}, \sigma) = \sqrt{[\varepsilon^{+}_{-}(\mathbf{k}, \sigma)]^2 + \left[\Delta^s_{\sigma\sigma}\right]^2}.$$

According to BCS theory, as long as $J_{ll'} < 0$ or ferromagnetic coupling, there exists a finite SC gap or order parameter to the gap equation.

The BCS-like gap equation for $S_A(l = 1) = -S_A(l = -1)$ is analogous to Eq. (23). The distinction lies in the emergence of SC in the spin-singlet channel, where the s-wave gap function factor $\gamma^s = 1$, exhibiting $\mathcal{T}$ symmetry, and the interaction term $J_{ll'}/4$ in the spin-triplet channel is replaced by $-3J_{ll'}/4$ in the spin-singlet channel gap equation according to the decomposition Eq. (20). For $J_{ll'} > 0$ in antiferromagetic interlayer coupling, there exists a finite SC order parameter solution to the gap equation.

B. AB stacking

For comparison, the dispersion in the AB stacking, characterized by $S_A(l = 1) = -S_B(l = -1)$, is spin dependent, similar to that in the single layer. The spin dependent dispersion is

$$\varepsilon^{\mp}_{+}(\mathbf{k}, \sigma) = \epsilon_{A+B}(\mathbf{k}) \mp \sqrt{[\epsilon_{AB}(\mathbf{k}) \mp t_\perp]^2 + [\epsilon_{A-B}(\mathbf{k}) - \sigma h]^2}. \tag{24}$$

Though the antiferromagnetic spin coupling is capable of facilitating spin-singlet pairing the energy dispersion $\varepsilon^{\mp}_{+}(\mathbf{k}, \uparrow) \neq \varepsilon^{\mp}_{+}(-\mathbf{k}, \downarrow)$ is unfavorable for the spin-singlet pairing formation, as in single-layer AM.

Finally, the energy dispersion relation for the AB stacking configuration with $S_A(l = 1) = S_B(l = -1)$ is given by

$$\varepsilon^{\mp}_{+}(\mathbf{k}, \sigma) = \epsilon_{A+B}(\mathbf{k}) \mp \sqrt{\epsilon^2_{A-B}(\mathbf{k}) + \xi^2_{\mp}(\mathbf{k})}, \tag{25}$$

with

$$\begin{aligned}\xi^2_{\mp}(\mathbf{k}) = &\epsilon^2_{AB}(\mathbf{k}) + t^2_\perp + h^2 \\ &\mp 2\sqrt{\left[\epsilon^2_{A-B}(\mathbf{k}) + t^2_\perp\right]h^2 + \epsilon^2_{AB}(\mathbf{k})t^2_\perp}.\end{aligned} \tag{26}$$

The stacking restores $\mathcal{T}$ symmetry, thereby resulting in $\varepsilon^{\mp}_{+}(\mathbf{k}, \uparrow) = \varepsilon^{\mp}_{+}(-\mathbf{k}, \downarrow)$ and the energy dispersion that is independent of spin. The electronic structure is capable of supporting both spin singlet and triplet Cooper pairing between layers. However, the ferromagnetic interlayer spin fluctuations selectively enhance spin-triplet pairing between layers.

IV. DISCUSSION AND CONCLUSION

In our model, we have ignored the spin-orbit coupling (SOC), electron-phonon interaction, long-range interlayer coupling, and twist angle between the layers. Although omitting SOC is a simplification often made in both the Hubbard and $t - J$ models the SOC breaks parity symmetry and could induce a mixture of spin singlet and triplet pairing and reconstruction of the Fermi surface. Electron-phonon interaction could be conducive to the SC pairing. Considering the experimental realization of the 2D single-layer and stacked AM models, a direct method is to exfoliate single or

double layers from these crystals and artificially assemble the sheets. Presently, more than a dozen AM candidates have been suggested [2]. The crystals with planar spin-momentum locking, such as La_2CuO_4, $FeSb_2$, KRu_4O_8, RuO_2, MnO_2, and MnF_2, are the optimal candidates for exfoliating and assembling operations.

To summarize, our study has investigated the energy dispersion in both single and stacked layer AM materials. Using a 2D anisotropic Hubbard model, we have analytically derived the general energy dispersions using the mean field method. In the single AM sheet, due to $\mathcal{T}$ symmetry broken, the energy dispersion is spin-polarized and only spin-triplet SC is favored. In contrast, the spin fluctuations typically favor spin-singlet pairing, as the AM order often slightly deviates from that in AFM. The discord between electronic structure and pairing interaction hinders SC formation in AM. Thus we demonstrate that stacking AM sheets could change the original symmetries present in the monolayer and interlayer magnetic coupling can enhance the low $\mathbf{q}$ spin fluctuations. The stacking could make both the electronic structure and spin fluctuations favor the formations of SC including spin singlet and triplet pairings, depending on stacking patterns. In the twisted bilayer AM layers, the unit cell expands, complicating the interlayer coupling which becomes spatially dependent rather than uniform. We further propose that twisted bilayer AM sheets could give rise to additional novel electronic properties, such as topology, flat bands, and collective excitations. Our work indicates that stacking sheets of AM materials could provide a unique platform for exploring new quantum phenomena. Modifying the electronic properties by turning the twist angle between AM sheets could lead to the development of novel electronic devices.

ACKNOWLEDGMENTS

We are thankful to Y. Wang for fruitful discussions. This work is supported by the National Natural Science Foundation of China (Grants No. 12174168, No. 12247101, No. 12274187, No. 11874188, No. 12047501, and No. 11874075), Science Challenge Project No. U1930401, and National Key Research and Development Program of China (Grant No. 2018YFA0305703).

[1] S. Hayami, Y. Yanagi, and H. Kusunose, Momentum-dependent spin splitting by collinear antiferromagnetic ordering, J. Phys. Soc. Jpn. **88**, 123702 (2019).

[2] L. Šmejkal, J. Sinova, and T. Jungwirth, Beyond conventional ferromagnetism and antiferromagnetism: A phase with nonrelativistic spin and crystal rotation symmetry, Phys. Rev. X **12**, 031042 (2022).

[3] S. Hayami, Y. Yanagi, and H. Kusunose, Bottom-up design of spin-split and reshaped electronic band structures in antiferromagnets without spin-orbit coupling: Procedure on the basis of augmented multipoles, Phys. Rev. B **102**, 144441 (2020).

[4] L. Smejkal, R. González-Hernández, T. Jungwirth, and J. Sinova, Crystal time-reversal symmetry breaking and spontaneous Hall effect in collinear antiferromagnets, Sci. Adv. **6**, eaaz8809 (2020).

[5] I. I. Mazin, K. Koepernik, M. D. Johannes, R. González-Hernández, and L. Šmejkal, Prediction of unconventional magnetism in doped $FeSb_2$, Proc. Natl. Acad. Sci. USA **118**, e2108924118 (2021).

[6] L.-D. Yuan, Z. Wang, J.-W. Luo, E. I. Rashba, and A. Zunger, Giant momentum-dependent spin splitting in centrosymmetric low-Z antiferromagnets, Phys. Rev. B **102**, 014422 (2020).

[7] V. Leeb, A. Mook, L. Šmejkal, and J. Knolle, Spontaneous formation of altermagnetism from orbital ordering, Phys. Rev. Lett. **132**, 236701 (2024).

[8] M. Roig, A. Kreisel, Y. Yu, B. M. Andersen, and D. F. Agterberg, Minimal models for altermagnetism, Phys. Rev. B **110**, 144412 (2024).

[9] L. Šmejkal, A. H. MacDonald, J. Sinova, S. Nakatsuji, and T. Jungwirth, Anomalous Hall antiferromagnets, Nat. Rev. Mater. **7**, 482 (2022).

[10] M. Naka, S. Hayami, H. Kusunose, Y. Yanagi, Y. Motome, and H. Seo, Anomalous Hall effect in κ-type organic antiferromagnets, Phys. Rev. B **102**, 075112 (2020).

[11] X. Zhou, W. Feng, X. Yang, G.-Y. Guo, and Y. Yao, Crystal chirality magneto-optical effects in collinear antiferromagnets, Phys. Rev. B **104**, 024401 (2021).

[12] K. Samanta, M. Ležaić, M. Merte, F. Freimuth, S. Blügel, and Y. Mokrousov, Crystal Hall and crystal magneto-optical effect in thin films of $SrRuO_3$, J. Appl. Phys. **127**, 213904 (2020).

[13] K.-H. Ahn, A. Hariki, K.-W. Lee, and J. Kuneš, Antiferromagnetism in RuO_2 as d-wave pomeranchuk instability, Phys. Rev. B **99**, 184432 (2019).

[14] M. Naka, S. Hayami, H. Kusunose, Y. Yanagi, Y. Motome, and H. Seo, Spin current generation in organic antiferromagnets, Nat. Commun. **10**, 4305 (2019).

[15] H.-Y. Ma, M. Hu, N. Li, J. Liu, W. Yao, J.-F. Jia, and J. Liu, Multifunctional antiferromagnetic materials with giant piezomagnetism and noncollinear spin current, Nat. Commun. **12**, 2846 (2021).

[16] R. González-Hernández, L. Šmejkal, K. Výborný, Y. Yahagi, J. Sinova, T. Jungwirth, and J. Železný, Efficient electrical spin splitter based on nonrelativistic collinear antiferromagnetism, Phys. Rev. Lett. **126**, 127701 (2021).

[17] D.-F. Shao, S.-H. Zhang, M. Li, C.-B. Eom, and E. Y. Tsymbal, Spin-neutral currents for spintronics, Nat. Commun. **12**, 7061 (2021).

[18] Q. Cui, B. Zeng, P. Cui, T. Yu, and H. Yang, Efficient spin seebeck and spin Nernst effects of magnons in altermagnets, Phys. Rev. B **108**, L180401 (2023).

[19] H. Bai, L. Han, X. Y. Feng, Y. J. Zhou, R. X. Su, Q. Wang, L. Y. Liao, W. X. Zhu, X. Z. Chen, F. Pan *et al.*, Observation of spin splitting torque in a collinear antiferromagnet RuO_2, Phys. Rev. Lett. **128**, 197202 (2022).

[20] L. Šmejkal, A. B. Hellenes, R. González-Hernández, J. Sinova, and T. Jungwirth, Giant and tunneling magnetoresistance in unconventional collinear antiferromagnets with nonrelativistic spin-momentum coupling, Phys. Rev. X **12**, 011028 (2022).

[21] T. Berlijn, P. C. Snijders, O. Delaire, H.-D. Zhou, T. A. Maier, H.-B. Cao, S.-X. Chi, M. Matsuda, Y. Wang, M. R. Koehler *et al.*, Itinerant antiferromagnetism in RuO_2, Phys. Rev. Lett. **118**, 077201 (2017).

[22] A. Bose, N. J. Schreiber, R. Jain, D.-F. Shao, H. P. Nair, J. Sun, X. S. Zhang, D. A. Muller, E. Y. Tsymbal, D. G. Schlom *et al.*, Tilted spin current generated by the collinear antiferromagnet ruthenium dioxide, Nat. Electron. **5**, 267 (2022).

[23] Z. Feng, X. Zhou, L. Šmejkal, L. Wu, Z. Zhu, H. Guo, R. González-Hernández, X. Wang, H. Yan, P. Qin *et al.*, An anomalous Hall effect in altermagnetic ruthenium dioxide, Nat. Electron. **5**, 735 (2022).

[24] O. Fedchenko, J. Minár, A. Akashdeep, S. W. D'Souza, D. Vasilyev, O. Tkach, L. Odenbreit, Q. Nguyen, D. Kutnyakhov, N. Wind *et al.*, Observation of time-reversal symmetry breaking in the band structure of altermagnetic RuO_2, Sci. Adv. **10**, eadj4883 (2024).

[25] I. Mazin, Editorial: Altermagnetism—a new punch line of fundamental magnetism, Phys. Rev. X **12**, 040002 (2022).

[26] S. Bhowal and N. A. Spaldin, Ferroically ordered magnetic octupoles in *d*-wave altermagnets, Phys. Rev. X **14**, 011019 (2024).

[27] S. López-Moreno, A. H. Romero, J. Mejía-López, and A. Muñoz, First-principles study of pressure-induced structural phase transitions in MnF_2, Phys. Chem. Chem. Phys. **18**, 33250 (2016).

[28] S. Lee, S. Lee, S. Jung, J. Jung, D. Kim, Y. Lee, B. Seok, J. Kim, B. G. Park, L. Šmejkal *et al.*, Broken Kramers degeneracy in altermagnetic mnte, Phys. Rev. Lett. **132**, 036702 (2024).

[29] T. Osumi, S. Souma, T. Aoyama, K. Yamauchi, A. Honma, K. Nakayama, T. Takahashi, K. Ohgushi, and T. Sato, Observation of a giant band splitting in altermagnetic mnte, Phys. Rev. B **109**, 115102 (2024).

[30] J. Krempaský, L. Šmejkal, S. W. D'Souza, M. Hajlaoui, G. Springholz, K. Uhlířová, F. Alarab, P. C. Constantinou, V. Strocov, D. Usanov *et al.*, Altermagnetic lifting of kramers spin degeneracy, Nature (London) **626**, 517 (2024).

[31] H. Reichlová, R. L. Seeger, R. González-Hernández, I. Kounta, R. Schlitz, D. Kriegner, P. Ritzinger, M. Lammel, M. Leiviskä, V. Petříček *et al.*, Macroscopic time reversal symmetry breaking by staggered spin-momentum interaction, arXiv:2012.15651.

[32] S. Reimers, L. Odenbreit, L. Šmejkal, V. N. Strocov, P. Constantinou, A. B. Hellenes, R. J. Ubiergo, W. H. Campos, V. K. Bharadwaj, A. Chakraborty *et al.*, Direct observation of altermagnetic band splitting in CrSb thin films, Nat. Commun. **15**, 2116 (2024).

[33] I. I. Mazin, Notes on altermagnetism and superconductivity, arXiv:2203.05000.

[34] D. Zhu, Z.-Y. Zhuang, Z. Wu, and Z. Yan, Topological superconductivity in two-dimensional altermagnetic metals, Phys. Rev. B **108**, 184505 (2023).

[35] C. W. J. Beenakker and T. Vakhtel, Phase-shifted Andreev levels in an altermagnet Josephson junction, Phys. Rev. B **108**, 075425 (2023).

[36] B. Brekke, A. Brataas, and A. Sudbø, Two-dimensional altermagnets: Superconductivity in a minimal microscopic model, Phys. Rev. B **108**, 224421 (2023).

[37] S.-B. Zhang, L.-H. Hu, and T. Neupert, Finite-momentum cooper pairing in proximitized altermagnets, Nat. Commun. **15**, 1801 (2024).

[38] S. A. A. Ghorashi, T. L. Hughes, and J. Cano, Altermagnetic routes to Majorana modes in zero net magnetization, Phys. Rev. Lett. **133**, 106601 (2024).

[39] Y.-X. Li and C.-C. Liu, Majorana corner modes and tunable patterns in an altermagnet heterostructure, Phys. Rev. B **108**, 205410 (2023).

[40] A. Bose, S. Vadnais, and A. Paramekanti, Altermagnetism and superconductivity in a multiorbital $t-J$ model, Phys. Rev. B **110**, 205120 (2024).

[41] D. Chakraborty and A. M. Black-Schaffer, Constraints on superconducting pairing in altermagnets, arXiv:2408.03999.

[42] S. B. Hong, M. J. Park, and K.-M. Kim, Unconventional *p*-wave and finite-momentum superconductivity induced by altermagnetism through the formation of Bogoliubov Fermi surface, Phys. Rev. B **111**, 054501 (2025).

[43] T. A. Maier and S. Okamoto, Weak-coupling theory of neutron scattering as a probe of altermagnetism, Phys. Rev. B **108**, L100402 (2023).

[44] P. Das, V. Leeb, J. Knolle, and M. Knap, Realizing altermagnetism in Fermi-Hubbard models with ultracold atoms, Phys. Rev. Lett. **132**, 263402 (2024).

[45] S. Giuli, C. Mejuto-Zaera, and M. Capone, Altermagnetism from interaction-driven itinerant magnetism, Phys. Rev. B **111**, L020401 (2025).

[46] L. D. Re, Dirac points and topological phases in correlated altermagnets, arXiv:2408.14288.

[47] Y. Cao, V. Fatemi, S. Fang, K. Watanabe, T. Taniguchi, E. Kaxiras, and P. Jarillo-Herrero, Unconventional superconductivity in magic-angle graphene superlattices, Nature (London) **556**, 43 (2018).

[48] J. Kang and O. Vafek, Symmetry, maximally localized wannier states, and a low-energy model for twisted bilayer graphene narrow bands, Phys. Rev. X **8**, 031088 (2018).

[49] J. M. B. L. dos Santos, N. M. R. Peres, and A. H. C. Neto, Graphene bilayer with a twist: Electronic structure, Phys. Rev. Lett. **99**, 256802 (2007).

[50] E. J. Mele, Commensuration and interlayer coherence in twisted bilayer graphene, Phys. Rev. B **81**, 161405(R) (2010).

[51] E. S. Morell, J. D. Correa, P. Vargas, M. Pacheco, and Z. Barticevic, Flat bands in slightly twisted bilayer graphene: Tight-binding calculations, Phys. Rev. B **82**, 121407(R) (2010).

[52] R. Bistritzer and A. H. MacDonald, Moiré bands in twisted double-layer graphene, Proc. Natl. Acad. Sci. USA **108**, 12233 (2011).

[53] X. Chen, J. Ren, Y. Zhu, Y. Yu, A. Zhang, P. Liu, J. Li, Y. Liu, C. Li, and Q. Liu, Enumeration and representation theory of spin space groups, Phys. Rev. X **14**, 031038 (2024).

[54] P. W. Anderson, Antiferromagnetism. Theory of superexchange interaction, Phys. Rev. **79**, 350 (1950).

[55] J. B. Goodenough, Theory of the role of covalence in the perovskite-type manganites [La, M(II)]MnO_3, Phys. Rev. **100**, 564 (1955).

[56] J. Kanamori, Theory of the magnetic properties of ferrous and cobaltous oxides, I, Prog. Theor. Phys. **17**, 177 (1957).

[57] J. Kanamori, Theory of the magnetic properties of ferrous and cobaltous oxides, II, Prog. Theor. Phys. **17**, 197 (1957).

[58] J. Chang, I. Eremin, P. Thalmeier, and P. Fulde, Theory of magnetic excitons in the heavy-fermion superconductor UPd_2Al_3, Phys. Rev. B **75**, 024503 (2007).

[59] C. Lu, Z. Pan, F. Yang, and C. Wu, Interlayer-coupling-driven high-temperature superconductivity in $La_3Ni_2O_7$ under pressure, Phys. Rev. Lett. **132**, 146002 (2024).

[60] J. Chang and J. Zhao, Theory of dual fermion superconductivity in hole-doped cuprates, Eur. Phys. J. B **90**, 154 (2017).